Heterogeneous Diffusion in a Reversible Gel

Pablo I. Hurtado,[1,2] Ludovic Berthier,[1] and Walter Kob[1]

[1]*Laboratoire des Colloïdes, Verres et Nanomatériaux, UMR 5587, Université Montpellier II and CNRS, Montpellier 34095, France*
[2]*Departamento de Electromagnetismo y Física de la Materia, and Instituto Carlos I de Física Teórica y Computacional, Universidad de Granada, Granada 18071, Spain*

(Received 20 December 2006; published 28 March 2007)

We introduce a microscopically realistic model of a physical gel and use computer simulations to study its static and dynamic properties at thermal equilibrium. The phase diagram comprises a sol phase, a coexistence region ending at a critical point, a gelation line determined by geometric percolation, and an equilibrium gel phase unrelated to phase separation. The global structure of the gel is homogeneous, but the stress is only supported by a fractal network. The gel dynamics is highly heterogeneous and we propose a theoretical model to quantitatively describe dynamic heterogeneity in gels. We elucidate several differences between the dynamics of gels and that of glass formers.

DOI: 10.1103/PhysRevLett.98.135503 PACS numbers: 61.43.Bn, 61.20.Lc, 82.70.Gg

Although gels are commonly used in everyday life, they continue to offer fundamental challenges to research. Their physics is determined by a wide window of length scales, from the molecular size of particles in the solvent to macroscopic structures, and by a similarly broad range of time scales: gels are ''complex'' fluids [1]. Of particular interest are physical gels which are typically made of molecules forming a stress-sustaining network, with links that have a finite lifetime, as opposed to chemical gels where junctions are permanent and properties follow directly from geometry. The transient character of the network in physical gels results in a complex interplay between structure and dynamics, leading to nontrivial flow properties. Here we propose a model of a reversible physical gel which is microscopically realistic (we are in fact inspired by one particular material), and specifically design a hybrid Monte Carlo and molecular dynamics numerical approach to successfully bridge the gap between microscopic details and macroscopic observations, while offering deep insight on the nature of physical gels.

Inspired by recent experimental work on gelation, a variety of ''minimal'' models have recently been studied to elucidate the connection between gelation and seemingly related phenomena: geometric percolation [2,3], glass transition [4–6], and phase separation [7,8]. Detailed experiments performed with colloidal particles with tunable interactions [9] revealed that a nontrivial interplay between phase separation and kinetic arrest may produce gel-like structures. Associating polymers constitute another well-studied example of reversible gels [1]. In that case, gels can be obtained far from phase separation, producing viscoelastic materials with highly nonlinear rheological properties that are not well understood [10,11]. In many cases, a close similarity between gelation and glass formation is reported [1]. We explain below this similarity but discuss also important differences.

Our model is inspired by a material described in Ref. [11]. It is a microemulsion of stable and monodisperse oil droplets in water mixed with telechelic polymers, i.e., long hydrophilic chains with hydrophobic end caps. A polymer can form a loop around a single droplet, or, more interestingly, a bridge between two droplets. Figure 1 is a snapshot taken from our simulations showing droplets and bridging polymers. For sufficiently high polymer concentrations, a percolating network can be formed (shown in light gray) and the system becomes a soft solid. However, thermally activated extraction of the hydrophobic heads leads to a slow reorganization of the network structure, and the material eventually flows at long times [12]. This material is interesting because functionality, lifetime of the bonds, volume fraction, and strength of the networks can all be adjusted independently, which is not always possible in attractive colloids [9], or in previous model systems, unless specific *ad hoc* assumptions are made [4–7]. Modeling such a complicated self-assembly is a challenge because of the wide range of scales involved. In our model, we neglect the solvent and include polymers and droplets as the elementary objects. Moreover, since the internal dynamics of the polymers is much faster than the gel dynamics, we coarse grain the polymer description and only retain their effect as links inducing an effective entropic interaction between the two droplets they connect. Coarse graining is a crucial step for efficient large scale simulations, not used in previous models [13].

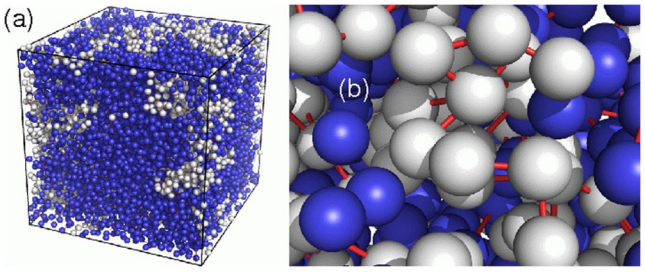

FIG. 1 (color online). (a) Structure of the physical gel for $\phi = 0.2$, $R = 2$, and $N = 10^4$. A percolating (light gray) cluster of droplets connected by telechelic (red) polymers, through which the remaining (dark blue) droplets can diffuse; see zoom in (b).

We consider an assembly of N droplets of diameter σ and mass m, interacting, in the absence of polymers, with a pair potential typical of soft spheres, $V_1(r_{ij}) = \epsilon_1(\sigma/r_{ij})^{14}$, where r_{ij} is the distance between droplets i and j, and ϵ_1 an energy scale. The potential is cut off and regularized at a finite distance, 2.5σ. In addition, N_p polymers of maximal extension ℓ can form bridges between droplets or loops. Polymer loops have an energy cost ϵ_0, but no effect on droplet dynamics. On the other hand, bridging polymers induce an entropic attraction between connected droplets, which we model using the classic finitely extensible nonlinear elastic form, $V_2(r_{ij}) = -\epsilon_2 \ln[1 - (r_{ij} - \sigma)^2/\ell^2]$, so that polymers act as springs at small elongation, but cannot become longer than ℓ. A configuration is specified by the droplets positions and velocities, $\{\mathbf{r}_i(t), \mathbf{v}_i(t)\}$, and by the polymer $N \times N$ connectivity matrix, $\{C_{ij}\}$, where C_{ij} is the number of polymers connecting droplets i and j. Summarizing, the Hamiltonian is thus

$$\mathcal{H} = \sum_{i=1}^{N}\left(\frac{m}{2}\mathbf{v}_i^2 + C_{ii}\epsilon_0 + \sum_{j>i}[V_1(r_{ij}) + C_{ij}V_2(r_{ij})]\right). \quad (1)$$

Simulation proceeds by solving Newton's equations for the droplets. Length scales are given in units of σ, energy in units of ϵ_1, and times in units of $\sqrt{m\sigma^2/\epsilon_1}$. We use the velocity Verlet algorithm with discretization $h = 0.005$. Simultaneously, we use Monte Carlo dynamics to evolve polymers. In an elementary move, a polymer is chosen at random, and one of its end caps is moved to a randomly chosen neighboring droplet. This proposed move is accepted with rate $\tau_{\text{link}}^{-1} \min[1, \exp(-\Delta V_2/T)]$, where ΔV_2 is the potential energy change during the move, T is the temperature, and τ_{link} controls the time scale for polymer rearrangements. In experiments τ_{link} has an Arrhenius behavior associated to the excitation cost for polymer extraction. We set $\ell = 3.5\sigma$ [11], $T = 1$, $\epsilon_0 = 1$, and $\epsilon_2 = 50$. We found little influence of ϵ_2 on the phase diagram. The relevant control parameters are the droplet volume fraction, $\phi = \pi N/(6V)$, where V is the volume, the number of polymer heads per droplet, $R = 2N_p/N$, and τ_{link}, which has no influence on static properties. We performed simulations for a wide range of parameters, $R \in [0, 18]$, $\phi \in [0.01, 0.3]$, $\tau_{\text{link}} \in [1, 10^4]$, $N \in [10^3, 10^4]$.

The phase diagram, as obtained after a systematic exploration of the control parameter space, is shown in Fig. 2. Its topology is in good agreement with experiments in the range studied [11]. In the low-ϕ, low-R region, the system resembles a dilute assembly of soft spheres, and has simple-liquid properties: this is the sol phase. Increasing R increases the effective attraction between droplets, so that phase separation occurs at large R between a low-ϕ, low-R phase and a large-ϕ, large-R phase [14]. We detect phase coexistence from direct visualization and by measuring the static structure factor, $S(q) = \langle N^{-1}\sum_{jk} \exp[i\mathbf{q} \cdot (\mathbf{r}_j - \mathbf{r}_k)]\rangle$, which exhibits the typical q^{-4} behavior at small q. We observe both nucleation or spinodal regimes depending on the quench depth. Interestingly, we find that the kinetics of the phase separation is extremely slow, and that the obtained patterns are very similar to the ones observed experimentally in short-range attractive colloidal suspensions [9].

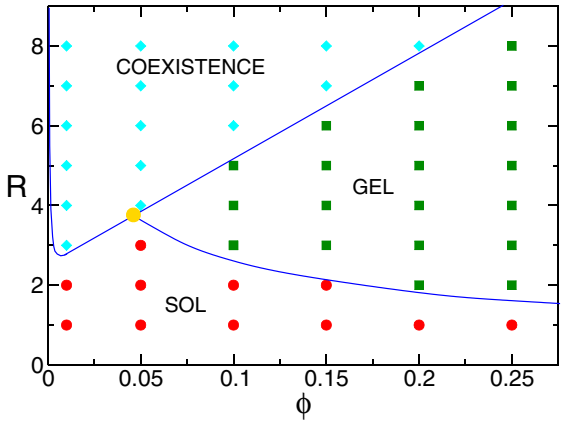

FIG. 2 (color online). Phase diagram for a wide range of volume fraction, ϕ, and number of polymer heads per droplet, R. Symbols are the investigated state points in the sol (○), gel (□), and phase separated (◇) regions; the yellow point is the approximate location of the critical point. Transition lines are sketched.

For $\phi > 0.05$, a broad gel region exists at thermal equilibrium between the sol phase at low-R and phase separation at large-R, see Fig. 2. In the gel phase, a system-spanning cluster of polymer-connected droplets emerges, which endows the fluid with viscoelastic properties, see Fig. 1. The sol-gel transition coincides with geometric percolation of polymer-connected clusters. Our gels are homogeneous, i.e., $S(q)$ remains typical of a simple fluid, as seen in experiments [11]. However, the spanning cluster is highly fractal near percolation and becomes thicker deeper in the gel phase. At percolation we find a distribution of cluster sizes $P(n) \sim n^{-\gamma}$, with $\gamma \approx 2.2$ compatible with random bond percolation, as seen in other systems [2,4,6,7]. Finally, the structure of the system becomes nontrivial when approaching the critical point, where $S(q)$ develops a power law behavior with an exponent close to -1.5 at small q for $\phi_c \approx 0.05$, $R_c \approx 3.5$.

We now show that the gel phase indeed behaves dynamically as a soft viscoelastic fluid. We have investigated the dynamics by measuring the self-intermediate scattering function, $F_s(q, t) = \langle N^{-1}\sum_j \exp\{i\mathbf{q} \cdot [\mathbf{r}_j(t) - \mathbf{r}_j(0)]\}\rangle$, and the mean-squared displacement, $\Delta^2(t) = \langle N^{-1}\sum_j |\mathbf{r}_j(t) - \mathbf{r}_j(0)|^2\rangle$. Figure 3(a) shows the evolution of $F_s(q, t)$ from the sol to the gel phase. While relaxation is fast and exponential in the sol phase, a slow secondary relaxation emerges at percolation. The final decay time varies little in the gel phase, but the height of the plateau at intermediate times evolves dramatically. A similar behavior is found for the coherent scattering function, as in experiments [11].

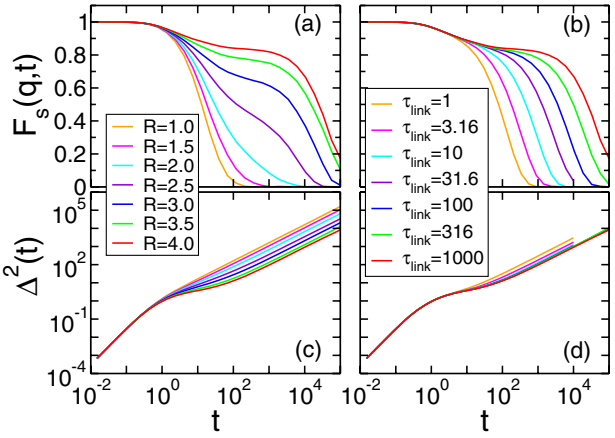

FIG. 3 (color online). Self-intermediate scattering function for $q = 0.46$ (a), (b) and mean-squared displacement (c), (d) for $N = 10^3$, $\phi = 0.2$. (a), (c) present the dynamics for $\tau_{\text{link}} = 10^3$ and several values of R across percolation ($R_p \approx 1.85$). Viscoelasticity continuously emerges at percolation. (b), (d) are for $R = 4$ and different values of τ_{link}, which directly controls the long-time decay of $F_s(q, t)$, while $\Delta^2(t)$ remains essentially unchanged.

Physically the plateau reflects the thermal vibrations of an elastic solid on intermediate time scale, while long-time decay reflects the flow of the system: the system is viscoelastic. In Fig. 3(b) we show that viscous flow is mostly controlled by τ_{link}, the rate for polymer extraction [2,15]. Flow in this system occurs when the percolating network slowly rearranges through polymer moves [12]. Therefore, gelation corresponds to the continuous emergence, for increasing polymer concentration, of a plateau in dynamic functions, with an almost constant relaxation time scale, controlled by the polymer dynamics. Gelation is thus qualitatively different from a glass transition where the plateau height remains constant with a dramatic increase of relaxation time scales [16]. Coincidence of gelation and percolation, put forward in [2] or dispelled in [7], happens whenever long-lived bonds make cluster restructuration very slow, but does not occur in systems where the bond lifetime is short at percolation [4].

Surprisingly, the mean-squared displacements shown in Fig. 3(c) and 3(d) appear as poor indicators of the dynamics. The comparison between Figures 3(b)–3(d) is in fact quite striking. While the final relaxation time scale, τ, in $F_s(q, t)$ scales roughly as τ_{link}, the diffusivity, D_s, extracted from the long-time behavior of $\Delta^2(t) \sim 6D_s t$ is almost constant. This is reminiscent of the "decoupling" phenomenon or "breakdown" of the Stokes-Einstein relation reported in supercooled fluids [16]. While "fractional" breakdown is reported in liquids, $D_s \sim \tau^{-\zeta}$, with ζ in the range 0.7–0.9 instead of the normal value $\zeta = 1$ [17], we find here $\zeta \approx 0$, quite an extreme case of decoupling. Decoupling in gels was reported in different systems [18].

In supercooled fluids, decoupling phenomena are commonly attributed to the existence of dynamic heterogeneity, that is, the existence of nontrivial spatiotemporal distributions of mobilities. The analogy is confirmed in Fig. 4 where we show distributions of droplet displacements, $G_s(r, t) = \langle N^{-1} \sum_i \delta(|\mathbf{r} - \mathbf{r}_i(t) + \mathbf{r}_i(0)|) \rangle$. Clearly, G_s exhibits a bimodal character suggesting coexistence of slow arrested droplets and fast diffusing droplets. Qualitatively similar distributions were reported in gels [5,9] and glasses [17,19]. Here, the snapshot in Fig. 1 suggests an obvious explanation for dynamic heterogeneity. At any given time, a system-spanning cluster of droplets which behaves as a solid on time scales smaller than τ_{link} coexists with droplets which can more freely diffuse through this arrested structure. We quantitatively confirm this interpretation in Fig. 4 where G_s is decomposed into two families of droplets: $G_s = c_A G_A + (1 - c_A) G_M$, where A (M) stands for droplets that are arrested (mobile) at time $t = 0$, c_A being the fraction of droplets belonging to the percolating cluster. While the central peak in G_s is dominated by G_A, the large "non-Gaussian" tails are dominated by G_M.

We now propose an analytic model to describe the dynamic heterogeneity of the gel, which incorporates the physical idea of a coexistence of a slow, percolating cluster of connected droplets and fast, more freely diffusing droplets, with a dynamic exchange between the two families set by polymer moves. Similar physical ideas were qualitatively discussed earlier [9,18,20], but were however not exploited within a quantitative model. We define $g_\alpha(\mathbf{r}, t)$, the probability that a droplet makes a displacement $\mathbf{r}$ in a time t provided it belongs to family α during the whole time interval $[0, t]$, $\alpha = A, M$. Let $p_\alpha(t)$ be the probability that a droplet in family α switches for the first time to the complementary family, $\bar{\alpha}$, at time t, and define $P_\alpha(t) \equiv \int_t^\infty p_\alpha(t')dt'$. Then we have

$$G_\alpha(\mathbf{r}, t) = P_\alpha(t) g_\alpha(\mathbf{r}, t) + \int_0^t dt' [\Delta_\alpha(\mathbf{r}, t') \circ G_{\bar{\alpha}}(\mathbf{r}, t - t')], \tag{2}$$

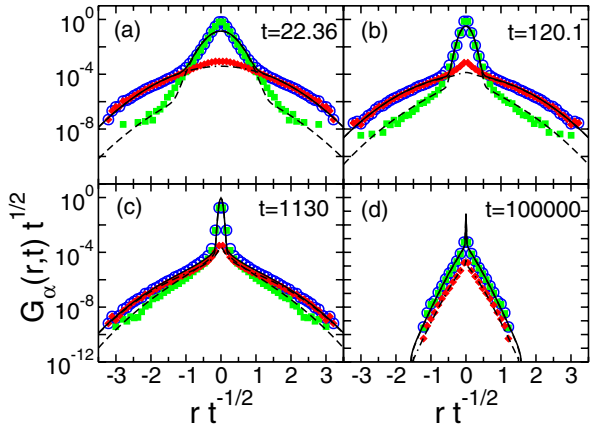

FIG. 4 (color online). Distribution of droplet displacements for $\phi = 0.2$, $R = 4$, $\tau_{\text{link}} = 100$ and different times for all droplets (○), and its decomposition over droplets that are initially free (◇) or arrested (□). Lines are from our model, Eq. (3).

where $\Delta_\alpha(\mathbf{r}, t) \equiv p_\alpha(t) g_\alpha(\mathbf{r}, t)$, and $\circ$ stands for spatial convolution. The first term describes droplets which persist in the same family between 0 and t, while the second term captures family exchanges. To keep the model simple, we assume the exchange dynamics to be homogeneous, with constant transition rates τ_α^{-1}, so $p_\alpha(t) = \exp(-t/\tau_\alpha)/\tau_\alpha$. In addition, stationarity implies that $c_A/\tau_A = (1 - c_A)/\tau_M$. The model can be solved analytically in the Fourier-Laplace domain:

$$G_\alpha(\mathbf{q}, s) = \frac{\tau_\alpha \Delta_\alpha(\mathbf{q}, s) + \tau_{\bar{\alpha}} \Delta_\alpha(\mathbf{q}, s) \Delta_{\bar{\alpha}}(\mathbf{q}, s)}{1 - \Delta_\alpha(\mathbf{q}, s) \Delta_{\bar{\alpha}}(\mathbf{q}, s)}. \quad (3)$$

To obtain analytic fits to the data we assume a Gaussian propagator for mobile droplets, $g_M(\mathbf{r}, t) = (4\pi D_M t)^{-3/2} \times \exp[-r^2/(4D_M t)]$, where D_M is an effective diffusivity. We treat the droplets attached to the cluster as localized in a bounded region of space of linear size a, which reflects the thermal vibrations of the elastic solid, $g_A(\mathbf{r}) = (\pi a^2)^{-3/2} \exp[-r^2/a^2]$. From Eq. (3) we thus obtain a simple (but lengthy) analytic expression for the self-intermediate scattering function $F_s(q, t)$ by inverse Laplace transform. We numerically invert the Fourier transform to get the displacement distributions. The free parameters of the model are $\{c_A, D_M, a, \tau_A\}$, but the first three parameters can be fixed by numerical observations. The concentration of droplets connected to the percolating cluster, $c_A \approx 0.94$, is directly measured. The value $D_M \approx 0.3$ is evaluated from an intermediate-time fit of $\Delta_M^2(t)$ restricted to initially mobile droplets. The localization length, $a \approx 1.79$, is similarly estimated from the plateau in $\Delta_A^2(t)$ restricted to droplets initially belonging to the percolating cluster. To get the excellent fits shown in Fig. 4, we adjust $\tau_A = 2 \times 10^4$, which coincides well with the time scale at which $\Delta_A^2(t)$ becomes diffusive, a physically sound definition for the average exchange time.

We were able to fit data for a wide range of parameters and find that our model performs similarly well for other state points. From Eq. (3), it is easy to predict that $\tau \propto \tau_A$, while $D_s = (1 - c_A) D_M + c_A a^2/(4\tau_A)$, in quantitative agreement with the decoupling data reported in Fig. 3, leading to $\zeta = 0$ for large τ_{link}. The diffusion constant is in fact entirely dominated by those droplets which do not contribute to viscoelasticity, and is therefore a poor indicator of the gel dynamics. These results show that dynamic heterogeneity in gels can be stronger than in supercooled fluids, but its origin is also much simpler: the system structure is heterogeneous, Fig. 1, while no such static structure exists in glasses.

Although motivated by a specific material, the new model for reversible gelation proposed in this work sheds light on the microscopic aspects of gelation and the heterogeneous dynamics of gel-forming systems. Moreover, our numerical findings motivated a simple yet accurate analytic modeling of dynamic heterogeneity, which is generally applicable to gels. Although slow and heterogeneous dynamics are superficially reminiscent of the physics of supercooled fluids, we discussed several qualitative differences between gels and glasses.

Discussions with G. Porte, C. Ligoure, and S. Mora motivated this work. We thank T. Bickel and S. Kumar for discussions, DYGLAGEMEM, MEyC No. FIS2005-00791, and Universidad de Granada for financial support.

[1] R. G. Larson, *The Structure and Rheology of Complex Fluids* (Oxford University Press, New York, 1999).
[2] E. Del Gado, A. Fierro, L. de Arcangelis, and A. Coniglio, Phys. Rev. E **69**, 051103 (2004).
[3] A. Hasmy and R. Jullien, Phys. Rev. E **53**, 1789 (1996).
[4] F. Sciortino, S. Mossa, E. Zaccarelli, and P. Tartaglia, Phys. Rev. Lett. **93**, 055701 (2004).
[5] A. M. Puertas, M. Fuchs, and M. E. Cates, Phys. Rev. Lett. **88**, 098301 (2002).
[6] E. Del Gado and W. Kob, Europhys. Lett. **72**, 1032 (2005).
[7] E. Zaccarelli, S. V. Buldyrev, E. La Nave, A. J. Moreno, I. Saika-Voivod, F. Sciortino, and P. Tartaglia, Phys. Rev. Lett. **94**, 218301 (2005).
[8] P. Charbonneau and D. R. Reichman, cond-mat/0604430.
[9] P. J. Lu, J. C. Conrad, H. M. Wyss, A. B. Schofield, and D. A. Weitz, Phys. Rev. Lett. **96**, 028306 (2006); S. Manley, H. M. Wyss, K. Miyazaki, J. C. Conrad, V. Trappe, L. J. Kaufman, D. R. Reichman, and D. A. Weitz, Phys. Rev. Lett. **95**, 238302 (2005); C. J. Dibble, M. Kogan, and M. J. Solomon, Phys. Rev. E **74**, 041403 (2006); A. I. Campbell, V. J. Anderson, J. S. van Duijneveldt, and P. Bartlett, Phys. Rev. Lett. **94**, 208301 (2005).
[10] T. Annable, R. Buscall, R. Ettelaie, and D. Whittlestone, J. Rheol. (N.Y.) **37**, 695 (1993); Y. Serero, R. Aznar, G. Porte, J. F. Berret, D. Calvet, A. Collet, and M. Viguier, Phys. Rev. Lett. **81**, 5584 (1998).
[11] E. Michel, M. Filali, R. Aznar, G. Porte, and J. Appell, Langmuir **16**, 8702 (2000).
[12] F. Tanaka and S. F. Edwards, Macromolecules **25**, 1516 (1992).
[13] P. G. Khalatur, A. R. Khokhlov, J. N. Kovalenko, and D. A. Mologin, J. Chem. Phys. **110**, 6039 (1999); S. K. Kumar and J. F. Douglas, Phys. Rev. Lett. **87**, 188301 (2001); T. Koga and F. Tanaka, Eur. Phys. J. E **17**, 115 (2005).
[14] A. Zilman, J. Kieffer, F. Molino, G. Porte, and S. A. Safran, Phys. Rev. Lett. **91**, 015901 (2003).
[15] I. Saika-Voivod, E. Zaccarelli, F. Sciortino, S. V. Buldyrev, and P. Tartaglia, Phys. Rev. E **70**, 041401 (2004).
[16] P. G. Debenedetti and F. H. Stillinger, Nature (London) **410**, 259 (2001).
[17] M. D. Ediger, Annu. Rev. Phys. Chem. **51**, 99 (2000).
[18] D. Bedrov, G. D. Smith, and J. F. Douglas, Europhys. Lett. **59**, 384 (2002); L. Guo and E. Luijten, J. Polym. Sci., Part B: Polym. Phys. **43**, 959 (2005).
[19] E. R. Weeks, J. C. Crocker, A. C. Levitt, A. Schofield, and D. A. Weitz, Science **287**, 627 (2000).
[20] A. M. Puertas, M. Fuchs, and M. E. Cates, J. Chem. Phys. **121**, 2813 (2004).